Letters

Undersea Simultaneous Wireless Power and Data Transfer System With Extended Communication Distance and High Rate

Tao Li, *Graduate Student Member, IEEE*, Zhichao Sun, *Student Member, IEEE*, Yijie Wang, *Senior Member, IEEE*, Jianwei Mai, *Member, IEEE*, and Dianguo Xu, *Fellow, IEEE*

***Abstract*—This letter proposes an undersea simultaneous wireless power and data transfer (SWPDT) system with extended communication distance and 1-Mb/s full-duplex communication. The proposed system operates in inductive power transfer-electric field communication mode, thus reducing the crosstalk between the power channel and communication channel. This letter proposes a novel communication channel construction method based on the single capacitor coupling principle, which can effectively extend the communication distance without additional mechanisms. The extended communication distance enables precommunication before charging and maintaining communication after completing charging, which is critical for undersea dynamic equipment. The resonant condition and transmission characteristics of the communication channel are analyzed. Two MHz communication bands are constructed to achieve full-duplex communication based on frequency division duplexing. Finally, the proposed undersea SWPDT prototype has a maximum output power of 1.2 kW and can maintain 1-Mb/s full-duplex communication within a range of 50 cm.**

***Index Terms*—Full duplex, simultaneous wireless power and data transfer (SWPDT) system, single capacitor coupled (SCC), undersea.**

I. Introduction

RELIABLE data exchange between the primary and secondary of the wireless power transfer (WPT) systems is crucial for realizing closed-loop control and monitoring system status [1], ultimately enhancing the efficiency and stability of undersea wireless charging.

Manuscript received 27 September 2023; revised 2 November 2023; accepted 22 November 2023. Date of publication 30 November 2023; date of current version 26 January 2024. This work was supported in part by the State Key Laboratory of Robotics and System (HIT) under Grant SKLRS-2022-ZM-15, in part by the Fundamental Research Funds for the Central Universities, in part by China National Postdoctoral Program for Innovative Talents under Grant BX20230479, and in part by China Postdoctoral Science Foundation under Grant 2023M730848. *(Corresponding author: Yijie Wang.)*

Tao Li, Zhichao Sun, Jianwei Mai, and Dianguo Xu are with the School of Electrical Engineering and Automation, Harbin Institute of Technology, Harbin 150006, China (e-mail: 22b306006@stu.hit.edu.cn; 23s006029@stu.hit.edu.cn; maijianwei@hit.edu.cn; xudiang@hit.edu.cn).

Yijie Wang is with the State Key Laboratory of Robotics and System, Harbin Institute of Technology, Harbin 150006, China (e-mail: wangyijie@hit.edu.cn).

Color versions of one or more figures in this article are available at https://doi.org/10.1109/TPEL.2023.3337801.

Digital Object Identifier 10.1109/TPEL.2023.3337801

However, conventional communication methods, such as 2.4G/5G modules, are difficult to meet the requirements of high data rate and low latency in undersea environments [2]. Simultaneous wireless power and data transfer (SWPDT) technology is a potential solution to these challenges.

In most SWPDT systems, data are transferred via near-field magnetic induction [3], [4], [5]. The magnetic induction link between the primary and secondary is established by multiplexing the power coils or adding additional coils. Through optimizing the data transceivers, full-duplex communication at Mb/s rates has become achievable [3]. However, limited by the decrease of the coupling coefficient, the transmission distance is smaller than the outer diameter of the coil.

In addition, data can also be transferred through the electric field [6], [7]. Two capacitors between the primary and secondary sides are constructed to form a loop for transferring data. The crosstalk is significantly reduced since power and data are transferred through different fields. Liu et al. [8] implemented a single capacitor coupled (SCC) WPT system. The self-capacitance and stray capacitances of the coupling plate are used to form a complete loop. However, it lacks advantages in terms of power and efficiency. SCC is more suitable to be used for transferring data undersea, which is not currently studied.

Considering the above challenges, especially the insufficient research on long-distance undersea SWPDT technology, this letter introduces an innovative solution to extend communication distance while maintaining high-speed full-duplex communication. The proposed system operates in the inductive power transfer-electric field communication (IPEC) mode. This letter is the first time to use the SCC principle to transfer data under seawater. The SCC-based communication channel forms loops by the parasitic capacitance between the power coils and the parasitic capacitance between the system and the ground or infinity. Without the need for additional mechanisms, the communication distance can be significantly extended, and the distance-to-diameter ratio (DDR) can also be improved while reducing the crosstalk between the power channel and the communication channel. Then, based on the analysis of the resonance conditions of the communication channel, two communication bands are constructed to achieve high-speed frequency-division-duplex (FDD) communication. Finally, to verify the feasibility of the proposed method, a 1.2-kW undersea SWPDT prototype with

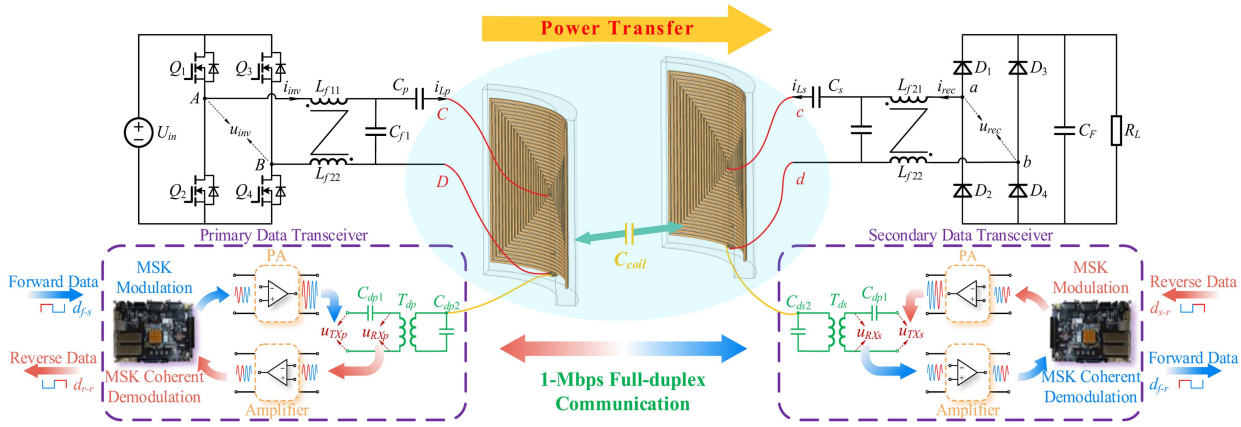

Fig. 1. Proposed undersea SWPDT system in IPEC mode.

1-Mb/s full-duplex communication is demonstrated. Moreover, the system can also maintain 1-Mb/s full-duplex communication at a distance of 50 cm.

II. System Overview

Fig. 1 depicts the schematic of the proposed undersea SWPDT system in IPEC mode. It comprises an inductive power channel and an SCC communication channel operating at 1-Mb/s full-duplex mode. Arc coupling coils are utilized to match the shell of undersea equipment. The capacitance between the coils is utilized for data transmission.

The power channel employs improved double-side *LCC* compensation topology [9]. The double-winding coupling compensation inductors are applied to further reduce the interference of the power channel on the communication channel [5].

The data channel utilizes primary and secondary data transceivers, incorporating modulation modules, coherent-demodulation modules, power amplifiers, capacitors, and transformers. These components are used to construct two MHz communication frequency bands, as detailed in Section III. Subsequently, the forward and reverse data signals, characterized by different frequencies, can be separated and identified through digital bandpass filters implemented by field programmable gate array (FPGA) to achieve FDD. Additionally, FPGA-based minimum shift keying (MSK) modulation and coherent demodulation techniques enhance spectral efficiency and communication rates.

III. Analysis of the Proposed System

This letter analyzes the principles of power transmission and data transmission of the system in Fig. 1.

A. Power Channel

According to the superposition theorem, the communication channel signal sources can be regarded as short circuits when analyzing the power channel. The power channel operates at 85 kHz. The parasitic capacitors of the system do not affect power transmission in this frequency band. Therefore, the power channel circuit can be obtained as shown in Fig. 2.

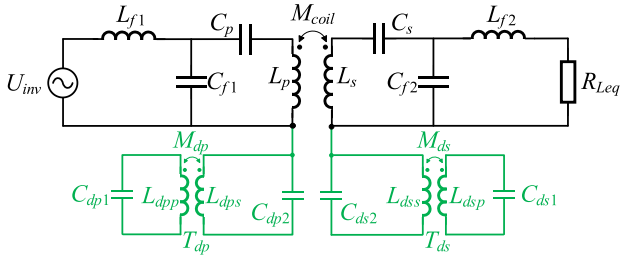

Fig. 2. Circuit of the power channel.

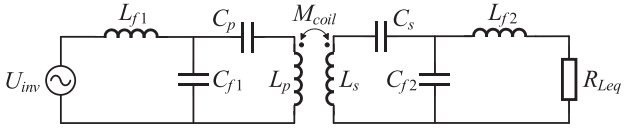

Fig. 3. Equivalent circuit of the power channel.

In Fig. 2, the communication channel and the power channel are connected at only a single point and do not form a complete loop. It can be considered that there is no current flowing into the communication channel from the power channel at the frequency. The impact of the communication channel on the power channel can be negligible. Therefore, the power channel can be equivalent to the double-side *LCC* circuit as shown in Fig. 3.

B. Communication Channel

Similarly, when analyzing the communication channel, the voltage source of the power channel can be considered as a short circuit. In the MHz frequency band, high-frequency displacement current can form a loop through the capacitance between coils and the stray capacitance of the system to infinity or ground. So, the data can be transferred through this loop bidirectionally. The communication channel circuit considering parasitic capacitance is shown in Fig. 4.

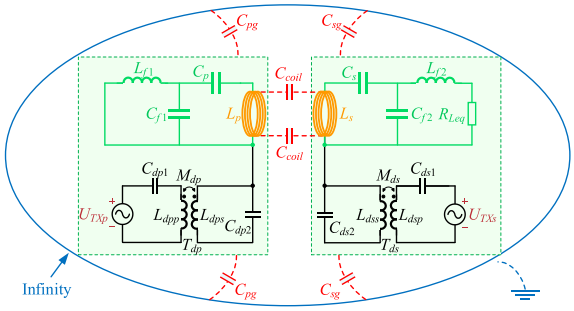

Fig. 4. Circuit of the communication channel.

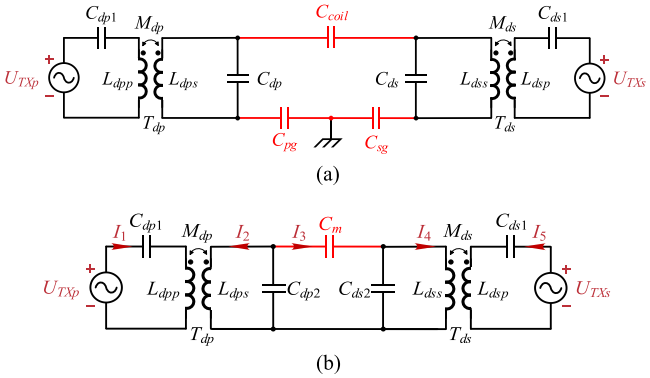

Fig. 5. Equivalent circuits of the communication channel. (a) Equivalent circuit. (b) Simplified equivalent circuit.

In the MHz frequency band, the impedance of the double-side *LCC* compensation is much smaller than the impedance of the capacitance between coils, so it can be regarded as a short circuit. Then, the equivalent circuit of the communication channel can be obtained as shown in Fig. 5(a). After further transforming, the circuit of Fig. 5(a) and (b) is obtained. C_m in Fig. 5(b) can be expressed as

$$C_m = \frac{1}{1/C_{\text{coil}} + 1/C_{pg} + 1/C_{sg}}. \tag{1}$$

To facilitate analysis and design, the communication channel circuit parameters in Fig. 5(b) are preset to be symmetrical, so that the forward and reverse transmission characteristics are the same. The specific parameter settings are as follows:

$$L_{dpp} = L_{dps} = L_{dss} = L_{dsp} = L_d \tag{2a}$$

$$M_{dp} = M_{ds} = M_d \tag{2b}$$

$$C_{dp1} = C_{dp2} = C_{ds2} = C_{ds1} = C_d. \tag{2c}$$

To extend the communication distance, the center frequencies and the amplitude of the received signal voltage should not change with the transmission distance, that is, the current I_3 flowing through C_m at the center frequencies should be independent of C_m. The circuit in Fig. 5(b) includes two frequencies that ensure I_3 is independent of C_m.

1) First Center Frequency ω_1: The transformers (T_{dp} and T_{ds}) in Fig. 5(b) are equivalent to the T-shaped circuit, as shown in Fig. 6(a). When L_d-M_d and C_d resonate at the frequency ω_1,

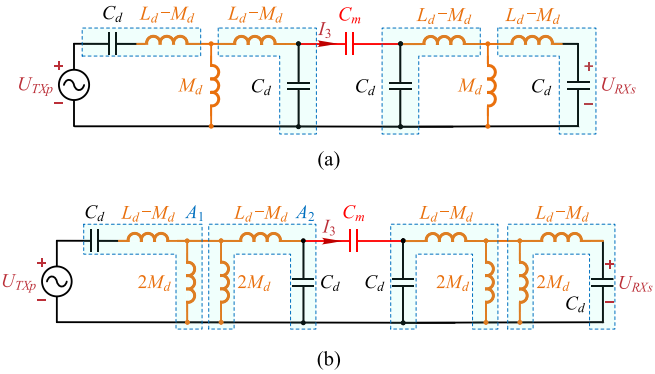

Fig. 6. Two resonance relationships in communication channels. (a) Circuit transformation of resonant frequency ω_1. (b) Circuit transformation of resonant frequency ω_2.

the current I_3 is independent of C_m. The expressions of ω_1 and I_3 can be calculated as

$$\omega_1 = \frac{1}{\sqrt{(L_d - M_d)\, C_d}},\ I_3 = \frac{\boldsymbol{U_{TXp}}}{j\omega_1 (L_d - M_d)}. \tag{3}$$

Since C_m does not appear in (3), ω_1 can be used as a center frequency of the communication band.

2) Second Center Frequency ω_2: The T-shaped circuit in Fig. 5(a) can also be equivalently transformed into Fig. 6(b). M_{d} is obtained by connecting two $2M_{\text{d}}$ in parallel. When loop A_1 and loop A_2 resonate at the frequency ω_2 simultaneously, the current I_3 is independent of C_m. The expressions of ω_2 and I_3 can be calculated as

$$\omega_2 = \frac{1}{\sqrt{(L_d + M_d)\, C_d}},\ I_3 = -\frac{\boldsymbol{U_{TXp}}}{j\omega_2 (L_d + M_d)}. \tag{4}$$

Since C_m does not appear in (4), ω_2 can also be used as a center frequency of the communication band.

In addition to the above two frequencies (ω_1 and ω_2), the other two frequencies can be obtained as follows:

$$\omega_3 = \sqrt{\frac{L_d\,(C_d^2 + 2C_dC_m - C_dC_m) - \sqrt{\zeta}}{C_d^2\,(C_d + 2C_m)\,(L_d^2 - M_d^2)}} \tag{5a}$$

$$\omega_4 = \sqrt{\frac{L_d\,(C_d^2 + 2C_dC_m - C_dC_m) + \sqrt{\zeta}}{C_d^2\,(C_d + 2C_m)\,(L_d^2 - M_d^2)}} \tag{5b}$$

where $\zeta = C_dC_m(2C_d^2M_d^2 - 4\,C_mC_dM_d^2 + C_dC_mL_d^2) + C_d^2 M_d^2\,(C_d + 2\,C_m)^2$.

The capacitance between coupling coils varying with distance under mediums of different conductivity is shown in Fig. 7. The conductivity of fresh water is 0.04 S/m. The conductivity of seawater is 4 S/m. Three observations can be made from this analysis. First, as the distance increases, the capacitance between the two coils gradually decreases and decreases faster in fresh water. Second, the capacitance in air is significantly lower than that in water due to the lower dielectric constant of air compared to water. Furthermore, the conductivity of the medium can also affect the capacitance of the coils over longer distances, resulting in higher capacitance in water with greater conductivity. The

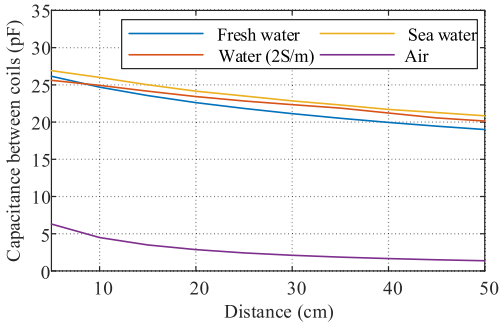

Fig. 7. Capacitance between coupling coils at different distances.

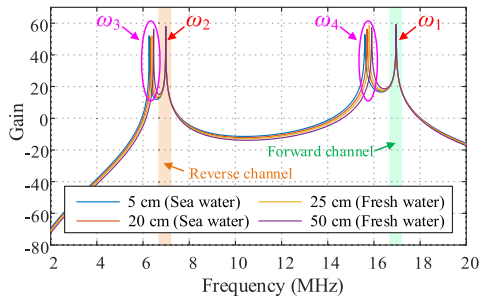

Fig. 8. Communication gain varies with frequency under different distances and mediums.

TABLE I
MAIN PARAMETERS UTILIZED IN EXPERIMENT

Symbol	Value	Symbol	Value
U_{in}	350 V	C_{f1}, C_{f2}	109 nF, 109.6 nF
f_p	85 kHz	C_p, C_s	212 nF, 191.5 nF
f_1	17 MHz	L_p, L_s	48.7 μH, 50.3 μH
f_2	8 MHz	L_d	2.64 μH
M_d	1.87 μH	C_d	115 pF

center frequencies of the communication frequency band are independent of C_m, ensuring that the system can operate effectively in different environments (including seawater, freshwater, and air).

From the circuit in Fig. 6, the transmission gain varying with frequency under different distances and mediums is shown in Fig. 8. Obviously, ω_3 and ω_4 change with the distance and medium. ω_1 and ω_2 are not affected by distance and medium, which is consistent with the results of (3) and (4). Therefore, to adapt to different distances and mediums, ω_1 and ω_2 are selected as the center frequencies. To achieve 1-Mb/s communication, the bandwidth needs 0.5 MHz using MSK modulation. Therefore, the forward band and reverse band are determined by the above analysis as marked in Fig. 8.

IV. EXPERIMENTAL VERIFICATION

The prototype is shown in Fig. 9, which shows the situation when the transmission distance is 50 cm. The conductivity of seawater is 4 S/m. Other parameters are listed in Table I.

In the experiment, SWPDT was tested at different distances, and the waveforms were recorded by the oscilloscope

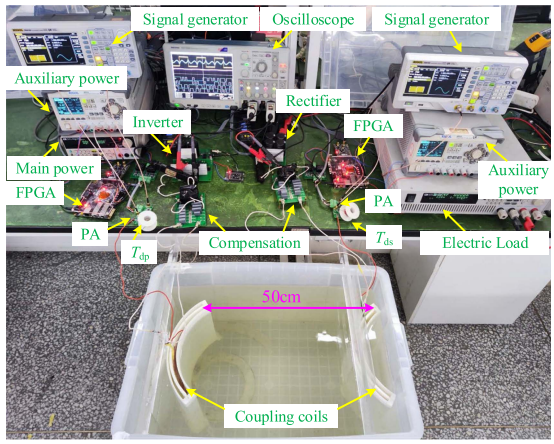

Fig. 9. Experimental prototype.

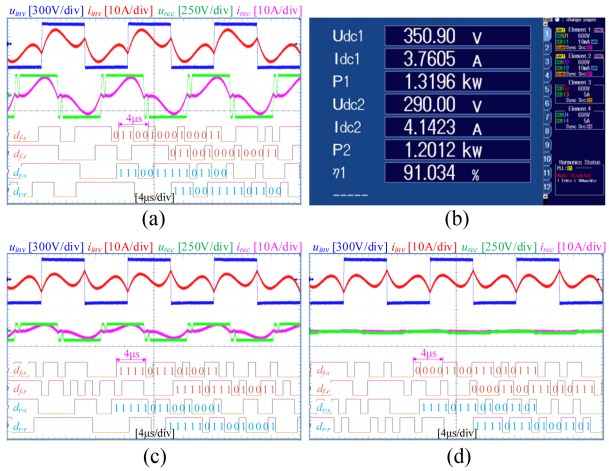

Fig. 10. Synchronous transmission of power and data at different distances. (a) 5 cm. (b) Power and efficiency at 5 cm. (c) 15 cm. (d) 50 cm.

MSO5204B with the logic probe P6616, as shown in Fig. 10. $u_{\rm inv}$ and $i_{\rm inv}$ are the voltage and current output of the inverter. $u_{\rm rec}$ and $i_{\rm rec}$ are the port voltage and current of the rectifier. *df-s* and *df-r* are the forward sending and receiving data, respectively. *dr-s* and *dr-r* are the reverse sending and receiving data, respectively.

The power transmission situation at different distances is as follows. At 5 cm, the system transfers power 1.2 kW with an efficiency of 91%. At 15 cm, the system transfers power 220 W. At 50 cm, the output power is very low. The reason for the rapid decrease in power is that as the distance increases, the coil coupling coefficient decreases rapidly.

Although the transmission power decreases rapidly as the distance increases, the system still maintains 1-Mb/s full-duplex communication all the time, as shown in Fig. 11. Especially, the DDR is 2 at 50 cm, and the system still operates at 1-Mb/s full-duplex communication. This verifies the method of extending communication distance.

The receiving port voltage waveforms and the communication data of the transceivers at 5 cm and 50 cm are shown in Fig. 11(a) and (b), respectively. There is no significant change in received

TABLE II
COMPARISON BETWEEN DIFFERENT STUDIES

Research	Medium	Maximum output power	Date rate	Maximum Communication distance / DDR
This	Seawater	1.2 kW	1 Mb/s /1 Mb/s	50 cm/2
[3]	Seawater	884 W	1 Mb/s/—	2 cm/0.1
[4]	Freshwater	1 kW	1 Mb/s/1 Mb/s	6 cm/0.27
[5]	Freshwater	518 W	500/700 kb/s	3 cm/0.1
[7]	Air	50 W	—/9.6 kb/s	2 cm/0.15

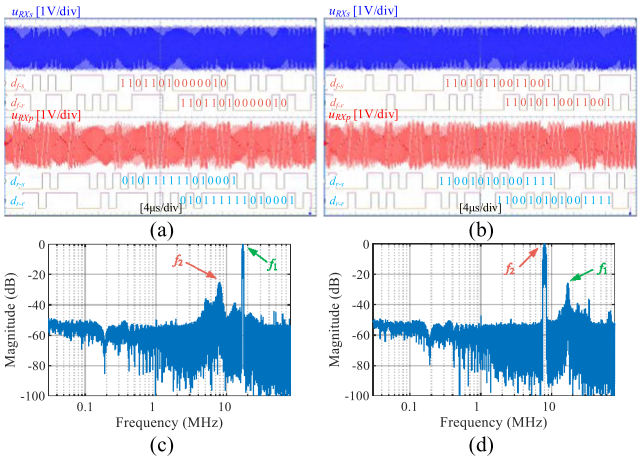

Fig. 11. Receiving port voltage waveforms and spectrum of the transceivers at different distances. (a) Waveforms at 5 cm. (b) Waveforms at 50 cm. (c) Spectrum of u_{RXs} at 50 cm. (d) Spectrum of u_{RXp} at 50 cm.

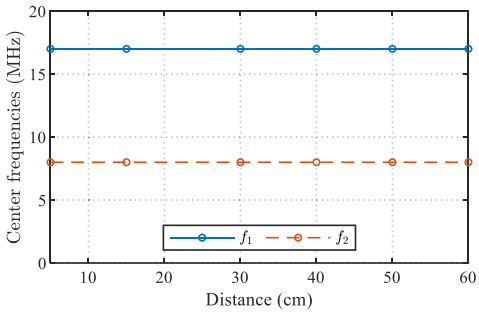

Fig. 12. Communication center frequencies at different distances.

signal amplitude at distances of 5 and 50 cm after Fourier analysis. The normalized spectrum of the received signal is shown in Fig. 11(c) and (d). The center frequencies of the forward channel and reverse channel are 17 MHz and 8 MHz, respectively. The crosstalk of the power channel to the communication channel is lower than −40 dB, which is consistent with the analysis in Section III. At 5 and 50 cm, the crosstalk between the two communication channels is lower than −20 dB, which shows that the channel has a high signal-to-noise ratio.

The variations of the forward transmission center frequency f_1 and the reverse transmission center frequency f_2 with transmission distance are shown in Fig. 12. Experimental results indicate that the two center frequencies remain unchanged at different transmission distances, which is consistent with the analysis in Section III.

Table II presents a comparative analysis between the proposed SWPDT system and the existing systems. This letter realizes 1-Mb/s bidirectional communication while achieving 1.2 kW power transfer. Notably, in contrast to previous systems, the proposed system exhibits a great enhancement in both communication distance, extending from less than 10 to 50 cm, and DDR, elevating from below 0.3 to 2.

V. CONCLUSION

This letter proposes an undersea SWPDT system with a 1-Mb/s full-duplex link operating in IPEC mode. The system establishes a novel communication channel based on the single capacitor coupling principle. The communication distance is significantly extended without additional mechanisms. Finally, 1-Mb/s full-duplex communication was achieved while transferring 1.2 kW power in parallel, and the 1-Mb/s full-duplex communication was maintained at a distance of twice the coil diameter in the experiment.

REFERENCES

[1] J. Liu, Z. Liu, and H. Su, "Passivity-based PI control for receiver side of dynamic wireless charging system in electric vehicles," *IEEE Trans. Ind. Electron.*, vol. 69, no. 1, pp. 783–794, Jan. 2022.
[2] Y. Yao, P. Sun, X. Liu, Y. Wang, and D. Xu, "Simultaneous wireless power and data transfer: A comprehensive review," *IEEE Trans. Power Electron.*, vol. 37, no. 3, pp. 3650–3667, Mar. 2022.
[3] C. Da, L. Wang, F. Li, C. Tao, and Y. Zhang, "Analysis of undersea simultaneous wireless power and 1 Mb/s data rate transfer system based on DDQ coil," *IEEE Trans. Power Electron.*, vol. 38, no. 10, pp. 11814–11825, Oct. 2023.
[4] T. Li, Z. Sun, Y. Wang, J. Mai, and D. Xu, "An underwater simultaneous wireless power and data transfer system with 1-Mbps full-duplex communication link," *IEEE Trans. Ind. Inform.*, to be published, doi: 10.1109/TII.2023.3295410.
[5] Y. Wang, T. Li, M. Zeng, J. Mai, P. Gu, and D. Xu, "An underwater simultaneous wireless power and data transfer system for AUV with high-rate full-duplex communication," *IEEE Trans. Power Electron.*, vol. 38, no. 1, pp. 619–633, Jan. 2023.
[6] X. Li, C. Tang, X. Dai, P. Deng, and Y. Su, "An inductive and capacitive combined parallel transmission of power and data for wireless power transfer systems," *IEEE Trans. Power Electron.*, vol. 33, no. 6, pp. 4980–4991, Jun. 2018.
[7] X. Yang et al., "A cost-effective implementation of independent data and power transmission channels in wireless power transfer systems," *IEEE Trans. Circuits Syst. II, Exp. Briefs*, vol. 69, no. 3, pp. 1532–1536, Mar. 2022.
[8] Z. Liu, Y. Su, H. Hu, Z. Deng, and R. Deng, "Research on transfer mechanism and power improvement technology of the SCC-WPT system," *IEEE Trans. Power Electron.*, vol. 38, no. 1, pp. 1324–1335, Jan. 2023.
[9] W. V. Wang, D. J. Thrimawithana, F. Lin, and G. A. Covic, "An MMC-based IPT system with integrated magnetics and ZVS operations," *IEEE Trans. Power Electron.*, vol. 37, no. 2, pp. 2425–2436, Feb. 2022.